



1 **Evaluation of air-soil temperature relationships**
2 **simulated by land surface models during winter across**
3 **the permafrost region**

4

5 **Wenli Wang¹⁺, Annette Rinke^{1,2+}, John C. Moore¹, Duoying Ji^{1*}, Xuefeng Cui³,**
6 **Shushi Peng^{4,17,18}, David M. Lawrence⁵, A. David McGuire⁶, Eleanor J. Burke⁷,**
7 **Xiaodong Chen⁸, Christine Delire⁹, Charles Koven¹⁰, Andrew MacDougall¹¹,**
8 **Kazuyuki Saito^{12,15}, Wenxin Zhang^{13,19}, Ramdane Alkama^{9,16}, Theodore J. Bohn⁸,**
9 **Philippe Ciais¹⁸, Bertrand Decharme⁹, Isabelle Gouttevin⁴, Tomohiro Hajima¹²,**
10 **Gerhard Krinner^{4,17}, Dennis P. Lettenmaier⁸, Paul A. Miller¹³, Benjamin Smith¹³,**
11 **Tetsuo Sueyoshi¹⁴**

12 ¹College of Global Change and Earth System Science, Beijing Normal University, Beijing,
13 China

14 ²Alfred Wegener Institute Helmholtz Centre for Polar and Marine Research (AWI), Potsdam,
15 Germany

16 ³School of System Science, Beijing Normal University, Beijing 100875, China

17 ⁴CNRS, LGGE, 38041 Grenoble, France

18 ⁵National Center for Atmospheric Research, Boulder, USA

19 ⁶U.S. Geological Survey, Alaska Cooperative Fish and Wildlife Research Unit, University of
20 Alaska Fairbanks, Fairbanks, AK, USA

21 ⁷Met Office Hadley Centre, Exeter, UK

22 ⁸School of Earth and Space Exploration, Arizona State University, Tempe, AZ, USA

23 ⁹GAME, Unit émixte de recherche CNRS/Meteo-France, Toulouse cedex, France

24 ¹⁰Lawrence Berkeley National Laboratory, Berkeley, CA, USA

25 ¹¹School of Earth and Ocean Sciences, University of Victoria, Victoria, BC, Canada



- 1 ¹²Japan Agency for Marine-Earth Science and Technology, Yokohama, Japan
- 2 ¹³Department of Physical Geography and Ecosystem Science, Lund University, Lund, Sweden
- 3 ¹⁴National Institute of Polar Research, Tachikawa, Japan
- 4 ¹⁵University of Alaska Fairbanks, Fairbanks, AK, USA
- 5 ¹⁶Institute for Environment and Sustainability (IES), Ispra, Italy
- 6 ¹⁷Université Grenoble Alpes, LGGE, 38041 Grenoble, France
- 7 ¹⁸LSCE, CEA/CNRS/UVSQ, Saclay, France
- 8 ¹⁹Center for Permafrost (CENPERM), Department of Geosciences and Natural Resource
- 9 Management, University of Copenhagen, DK-1350 Copenhagen, Denmark
- 10
- 11 + *these authors contributed equally to this work*
- 12 * *correspondence to:* Duoying Ji (duoyingji@bnu.edu.cn)
- 13



1 **Abstract.** A realistic simulation of snow cover and its thermal properties are important for
2 accurate modelling of permafrost. We analyze simulated relationships between air and near-
3 surface (20 cm) soil temperatures in the Northern Hemisphere permafrost region during winter,
4 with a particular focus on snow insulation effects in nine land surface models and compare
5 them with observations from 268 Russian stations. There are large across-model differences as
6 expressed by simulated differences between near-surface soil and air temperatures, (ΔT), of 3 to
7 14 K, in the gradients between soil and air temperatures (0.13 to 0.96 °C/°C), and in the
8 relationship between ΔT and snow depth. The observed relationship between ΔT and snow
9 depth can be used as a metric to evaluate the effects of each model's representation of snow
10 insulation, and hence guide improvements to the model's conceptual structure and process
11 parameterizations. Models with better performance apply multi-layer snow schemes and
12 consider complex snow processes. Some models show poor performance in representing snow
13 insulation due to underestimation of snow depth and/or overestimation of snow conductivity.
14 Generally, models identified as most acceptable with respect to snow insulation simulate
15 reasonable areas of near-surface permafrost (12-16 million km²). However, there is not a
16 simple relationship between the quality of the snow insulation in the acceptable models and the
17 simulated area of Northern Hemisphere near-surface permafrost, likely because several other
18 factors such as differences in the treatment of soil organic matter, soil hydrology, surface
19 energy calculations, and vegetation also provide important controls on simulated permafrost
20 distribution.



4

1 **1 Introduction**

2 Present-day permafrost simulations by global climate models are limited and future
3 projections contain high, model-induced uncertainty (e.g., Slater and Lawrence, 2013; Koven
4 et al., 2013). Most of the model biases and across-model differences in simulating permafrost
5 area are due to biased simulations of the atmosphere (air temperature, precipitation), land
6 (snow, soil temperature) and their coupling. In winter, the snow insulation effect is a key
7 process for the air-soil temperature coupling. Its strength depends on both the snow quantity
8 (depth, areal coverage) and snow quality (density, conductivity) (see overview by Zhang,
9 2005). Many individual model studies have shown the strong impact of a few snow
10 parameters on soil temperature simulations (e.g., recently, Dutra et al., 2012; Gouttevin et al.,
11 2012; Essery et al., 2013; Wang et al., 2013; Jafarov et al., 2014). Most importantly,
12 consideration of wet snow metamorphism and snow compaction, improved snow thermal
13 conductivity and multi-layer snow schemes improve the simulation of snow dynamics and
14 soil temperature. Parameterizations that take into account snow compaction (e.g. related to
15 overburden pressure, thermal metamorphism and liquid water) work better than simpler
16 schemes such as an exponential increase of density with time (Dutra et al., 2010). The
17 influence of snow thermal conductivity on soil regime has been demonstrated by many model
18 studies (e.g., Bartlett et al., 2006; Saha et al., 2006; Vavrus, 2007; Nicolsky et al., 2007;
19 Dankers et al., 2011; Gouttevin et al., 2012). Winter soil temperature can change by up to 20
20 K simply by varying the snow thermal conductivity by 0.1-0.5 W m⁻¹ K⁻¹ (Cook et al., 2008).
21 The snow insulation effect also plays an important role for the Arctic soil temperature
22 response to climate change (e.g., reduced soil warming due to shallower snow versus
23 enhanced soil warming due to shorter snow season) (e.g., Lawrence and Slater, 2010), and
24 therefore for future near-surface permafrost thawing and soil carbon vulnerability (e.g.,
25 Schuur et al., 2008). The model skill in atmosphere-soil coupling with the concomitant snow
26 cover in the Arctic is an important factor in the assessment of limitations and uncertainty of
27 carbon mobility estimates (Schaefer et al., 2011).

28

29 The Snow Model Intercomparison Project (Snow MIP) (Essery et al., 2009) and the Project
30 for Intercomparison of Land-Surface Parameterization Schemes (PILPS) Phase 2e (Slater et
31 al., 2001) examined the snow simulations of an ensemble of land-surface schemes for the
32 mid-latitudes. However, until now there has been no attempt to evaluate the air-soil
33 temperature relationship in the Northern Hemisphere permafrost region and the detailed role



5

1 of snow depth therein across an ensemble of models. In such an investigation, a first suitable
2 approach is the evaluation of stand-alone (off-line) land surface models (LSMs). The
3 retrospective (1960-2009) simulations from the model integration group of the Permafrost
4 Carbon Network ("PCN"; <http://www.permafrostcarbon.org>) provide an opportunity to
5 evaluate an ensemble of nine state-of-the-art LSMs. Here, the LSMs are run with observation-
6 based atmospheric forcing, meaning that snow depth is not influenced by biases in the
7 atmospheric forcing in a coupled model set-up. The evaluation of the offline modeled air
8 temperature - snow depth - near-surface soil temperature relationship in winter is therefore
9 important for revealing a model's skill in representing the effects of snow insulation.

10

11 Most of the LSMs participating in PCN are the land-surface modules of Earth System Models
12 (ESMs) participating in the Coupled Model Intercomparison Project (CMIP5; [http://cmip-
13 pcmdi.llnl.gov/cmip5/](http://cmip-pcmdi.llnl.gov/cmip5/)) although in some cases different versions were used for PCN and
14 CMIP5 simulations. Thus, the results we present can guide the corresponding evaluation of
15 these ESMs, though analysis of coupled model results requires consideration of couplings
16 between model components and is necessarily more complex.

17

18 The scope of the present study is to analyze the extent to which the ensemble of PCN models
19 can reproduce the observed relationship between air and near-surface soil temperatures in the
20 Northern Hemisphere permafrost region during winter, with a particular focus on the snow
21 insulation effect. For the latter we analyze the impact of snow depth on the difference
22 between near-surface soil and air temperatures. Our related key questions are: How well do
23 the models represent the observed magnitude and spatial pattern of the snow depth control
24 over the air-soil temperature difference in winter? What is the range of these simulated
25 relationships across the model ensemble? To the extent possible, we try to relate the
26 performance level to the model's snow schemes. With this aim in mind, a simultaneous
27 analysis of simulated air and near-surface soil temperatures, and snow depth is presented and
28 compared with those from a novel set of Russian station observations. We focus here on a
29 comprehensive Russian station data set because this has been compiled within PCN, and it is
30 hard to find other station data sets which provide simultaneous observations of both air and
31 soil temperatures as well as snow depth over a long period.

32

33 In Sect. 2, we describe the model simulations, the station observations used for evaluation,
34 and the analysis methods. In Sect. 3, we present a detailed analysis of near-surface air



6

1 temperature - snow depth - soil temperature relationships in winter. In Sect. 4, we discuss the
2 roles of atmospheric forcing and model processes. We summarize our findings and present
3 conclusions in Sect. 5.

4 **2 Data and Analysis**

5 **2.1 Models**

6 We use data from nine LSMs participating in the PCN, including CLM4.5, CoLM, ISBA,
7 JULES, LPJ-GUESS, MIROC-ESM, ORCHIDEE, UVic, and UW-VIC. For detailed
8 information about the models and simulations we refer to Rawlins et al. (2015) and Peng et al.
9 (2015). The total soil depth for soil thermal calculations ranges from 3 m (divided in 8 layers)
10 in LPJ-GUESS to 250 m (divided in 14 layers) in UVic. The soil physical properties differ
11 among the models as well, and four of them (CLM4.5, ISBA, UVic, UW-VIC) include
12 organic horizons. Three models (ISBA, LPJ-GUESS, UW-VIC) did not archive soil sub-grid
13 results and provide area-weighted ground temperature (i.e. averaged over wetlands and
14 vegetated areas, and in some cases lake fractions).

15

16 Table 1 lists relevant snow model details. One model (UVic) uses an implicit snow scheme
17 which replaces the upper soil column with snow-like properties, i.e. the near-surface soil layer
18 takes the temperature of the air-snow interface. The other models use separate snow layers on
19 top of the ground, either a single bucket (LPJ-GUESS, UW-VIC) or multi-layer snow
20 schemes (CLM4.5, CoLM, ISBA, JULES, MIROC-ESM, ORCHIDEE). Snow insulation is
21 explicitly considered in all models; increasing snow depth increases the insulation effect.
22 Many models consider the effect of varying snow density on insulation (Table 1). This is
23 parameterized by a snow conductivity-density relationship that describes how, as snow
24 density increases, thermal conductivity increases, thereby reducing the snow insulation. Some
25 of the models (LPJ-GUESS, MIROC-ESM, ORCHIDEE, UVic) use a fixed snow density,
26 consider only dry snow and no compaction effects, while others represent liquid water in
27 snow and different processes for snow densification such as mechanical compaction, and
28 thermal and destructive metamorphism (Table 1).

29

30 The simulations were generally run for the period 1960-2009, although some simulations
31 were stopped a few years earlier. Each model team was free to choose appropriate driving
32 data sets for weather and climate, atmospheric CO₂, nitrogen deposition, disturbance, land
33 cover, soil texture, etc. However, the climate forcing data (surface pressure, surface incident



7

1 longwave and shortwave radiation, near-surface air temperature, wind and specific humidity,
2 rain and snowfall rates) are from gridded observational datasets (e.g. CRUNCEP, WATCH)
3 (SI Table 1). The exception is MIROC-ESM, which was run as a fully-coupled model, forced
4 by its own simulated climate. Mean annual temperature of the MIROC-ESM simulations for
5 the permafrost region were within the range (-7.2 to 2.2 °C) of the other forcing data sets used
6 in this study and the trend in near-surface air temperature (+0.03 °C yr⁻¹) was the same for all
7 forcing data sets. However, MIROC-ESM had both the highest annual precipitation (range
8 433 to 686 mm) and the highest trend in annual precipitation (range -2.1 to +0.8 mm yr⁻¹)
9 among the forcing data sets.

10

11 The spatial domain of interest is the Northern Hemisphere permafrost land regions. Our
12 analysis is based on the 0.5° × 0.5° resolution gridded driving and modeled data for winter
13 (DJF) 1980-2000.

14 2.2 Observations

15 A data set of monthly near-surface air temperature, 20 cm soil temperatures and snow depth
16 from Russian meteorological stations have been provided by the All-Russian Research
17 Institute of Hydrometeorological Information-World Data Centre (RIHMI-WDC;
18 <http://meteo.ru/>) (Sherstyukov, 2008). 579 stations report snow depth and 268 stations provide
19 simultaneous data of all three variables. Ground surface temperature data are not available.
20 Precipitation station data have been compiled from the Global Summary of the Day (GSOD)
21 data set produced by the National Climatic Data Center (NCDC; <http://www.ncdc.noaa.gov>)
22 for all of the stations that are included in the RIHMI-WDC data set. We also use gridded
23 snow water equivalent (SWE) data from the GlobSnow-2 product
24 (<http://www.globsnow.info/swe/>), which has been produced using a combination of passive
25 microwave radiometer and ground-based weather station data (Takala et al., 2011). Snow
26 depth was then calculated from SWE using a snow density of 250 kg m⁻³. Orographic
27 complexity, vegetation cover, and snow state (e.g. wet snow) affect the accuracy of this
28 product. When compared with ground measurements, the GlobSnow product can show
29 regional differences (of ca. 0.5-5 cm) with biases increasing with increasing SWE (e.g.,
30 Takala et al., 2011; Muskett, 2012). All these data have been compiled for winter (DJF) and
31 the same time period of 1980-2000. This period was chosen because soil temperature data are
32 sparse before 1980 and the JULES simulation stopped in the year 2000. Comparison of the
33 simulations with the station data was done using a weighted bilinear interpolation from the 4
34 surrounding model grid points onto the station locations.



8

1 **2.3 Analysis Methods**

2 Our analysis is focused on the common winter (DJF) condition, although snow can begin in
3 November and end at the beginning of May, but we checked that a different winter definition
4 (NDJFMA) does not substantially change the results. The focus in our study is on the
5 evaluation of the simulated air-soil temperature relationships, modulated by snow depth. For
6 this, we analyze the winter mean as well as the interannual variability (expressed as the
7 standard deviation) of 4 variables: near-surface air temperature (T_{air}), near-surface soil
8 temperature (soil temperature at 20 cm depth; T_{soil}), snow depth (d_{snow}), and the difference
9 between T_{soil} and T_{air} . This difference ΔT ($\Delta T = T_{soil} - T_{air}$) is called the air-soil temperature
10 difference. By limiting our analysis to the winter only, we are able to attribute the across-
11 model and model-to-observation differences in ΔT primarily to snow insulation effects. We
12 assume that there is relatively little impact due to soil moisture and texture between surface
13 and 20 cm depth in winter. Although we recognize the difference between ground surface and
14 20 cm soil temperatures and that soil organic layer could play a role in certain locations (e.g.,
15 Romanovsky and Osterkamp, 1995), ground surface temperatures are not recorded in the
16 Russian data set, while 20 cm soil depth temperatures are, hence our choice. However, we
17 find that the results do not significantly change when the model simulated temperature
18 differences between ground surface and near-surface air temperature are used instead of
19 between 20 cm soil and near-surface air temperatures.

20

21 We use correlation analysis to investigate the co-variability between ΔT and d_{snow} as well as
22 between T_{soil} and its two forcing factors (T_{air} and d_{snow}). The input consists of detrended time
23 series of winter means at each grid point. The calculated correlation maps (i.e. spatial
24 distributions of correlation coefficients) based on model and observation data, allow the
25 comparison of the spatial patterns of these relationships. Significance of correlation
26 coefficients is estimated by the Student t-test.

27

28 To further examine the functional behavior between different variables, we present relation
29 diagrams between pairs of variables (e.g. variation of ΔT with change of d_{snow}). To evaluate
30 the performance of the individual LSMs we calculate the root-mean-square error (RMSE)
31 between the observed and modeled relationships. We illustrate the dependence on air
32 temperatures by evaluating the models and observations for several different near-surface air
33 temperature ranges. We split the data into 3 regimes: the coldest conditions ($T_{air} \leq -25$ °C)
34 represent 24% of observations, the intermediate temperature conditions (-25 °C < $T_{air} \leq -15$ °C)



9

1 represent 42% of the observations, and the warmest conditions ($-15\text{ °C} < T_{air} \leq -5\text{ °C}$) represent
2 34% of observations. The principal motivation for such classifications is to distinguish dry
3 snow pack regimes from those where sporadic melt may occur even in winter. Hence it is an
4 indirect separation of temperature-gradient metamorphosis regimes and density-gradient
5 metamorphosis snow pack regimes. Additionally, we present conditional probability density
6 functions (PDFs) of ΔT for different snow depth and air temperature regimes and compare the
7 simulated with those obtained from station observations.

8 **3 Results**

9 **3.1 Relationship between air – soil temperature difference and snow depth**

10 The air-soil temperature difference (ΔT) - snow depth (d_{snow}) relationship in winter (Fig. 1)
11 shows that observations and all models produce a clear relationship between increase of ΔT
12 and increases of d_{snow} . However, Fig. 1 also shows a wide across-model spread in the
13 simulated relationships, and that some of the models are not consistent with the behavior in
14 the observations. There is also significant scatter in the observation-based relationship, the
15 inter-quartile range of ΔT is 1.5-8.5 K at specific snow depth and air temperature regimes,
16 likely resulting from complicating factors such as snow pack density and moisture content
17 variability over the winter, as well as observational errors. Similar ranges of variability are
18 produced by several models (such as CLM4.5, CoLM and JULES), but other models (such as
19 ISBA and MIROC-ESM) produce noticeably smaller variations.

20

21 The Russian station data and some model results exhibit a linear relation between winter ΔT
22 and d_{snow} at relatively shallow snow depths with a trend towards asymptotic behavior at larger
23 snow depths (Fig. 1), which is in agreement with earlier findings (Zhang, 2005; Ge and Gong,
24 2010; Morse et al., 2011). However, only three models (CLM4.5, CoLM, JULES) reproduce
25 reasonably well the $\Delta T - d_{snow}$ relationship seen in the observational station data (Fig. 1) using
26 a benchmark of $RMSE < 5\text{ K}$ for all temperature regimes. In particular LPJ-GUESS,
27 ORCHIDEE, UVic, UW-VIC, MIROC-ESM show large RMSE for cold air conditions. ISBA
28 stands out overall, with a RMSE of 7-18 K in all temperature ranges. We conclude that these
29 models do not adequately represent the features of the observed $\Delta T / d_{snow}$ relationship.

30

31 Figure 2 views the $\Delta T / d_{snow}$ relationship in the complementary form of the PDFs of ΔT for
32 different snow depth and air temperature regimes. Since the Russian snow depths are clearly
33 non-Normal in distribution (SI Fig. 1, with a median d_{snow} of 30 cm), we divide the data into



10

1 "shallow" ($d_{snow} \leq 20$ cm) and "thick" ($d_{snow} \geq 45$ cm) regimes. The modal value of the station
2 data ΔT PDF is 5 K for "shallow" snow and 14 K for "thick" snow - that is thick snow is a
3 better insulator than thin snow. Based on the ΔT PDFs, five models (CoLM, CLM4.5, JULES,
4 ORCHIDEE, MIROC-ESM) successfully separate the ΔT regimes under different snow depth
5 conditions, while the other models clearly fail for at least one of these snow depth regimes.
6 However, even for the better models, both the shapes and the modal values of the simulated
7 PDFs differ from the observed PDF.

8

9 Both Figs. 1 and 2 indicate that air-soil temperature differences are related to air temperature
10 conditions. This is due to snow pack properties, particularly its density and moisture content,
11 that affect the air-soil temperature difference. For example, the density of fresh fallen snow
12 tends to be much lower under cold air temperatures than warm (Anderson, 1976), leading to
13 increased insulation (larger ΔT). Snow densification is also a function of air temperature, for
14 example, depth hoar metamorphosis of the snow pack, which produces more insulation
15 (loosely packed depth-hoar crystals have very low thermal conductivity), is promoted by
16 strong thermal gradients in the snow pack, and is typical of continental climates (e.g., Zhang
17 et al., 1996).

18

19 The observations in Figs. 1 and 2 indicate that snow under colder climates have greater
20 insulation than under warmer climates. This is shown by a larger ΔT for colder T_{air} than for
21 warmer T_{air} (for a certain snow depth) and a greater sensitivity of ΔT to changes in d_{snow} (Fig.
22 1), and by the larger modal value of the ΔT PDF for colder T_{air} than for warmer T_{air} (21 K for
23 $T_{air} \leq -25$ °C and 9 K for -15 °C $< T_{air} \leq -5$ °C; Fig. 2). This is consistent with colder climates
24 having lower density snow packs, and the differences are in line with measurements of snow
25 density variability (Zhong et al., 2013). Additionally, both the inter-quartile range in Fig. 1
26 and the width of the PDFs in Fig. 2 become larger as air temperatures cool. This may be
27 related to the formation of depth hoar, which is a very good insulator and its varying presence
28 in the snow pack decouples ΔT from d_{snow} . Cold, thin snow packs tend to contain much more
29 low density depth hoar than warmer snow packs (e.g., Zhang et al., 1996; Singh et al., 2011).
30 Continental regions have large annual temperature cycles, with greater interannual variability
31 and thinner snow packs, than maritime ones. This variability leads to greater scatter and
32 greater sensitivity of the $\Delta T/d_{snow}$ relationship in the cold winter regions. An additional cause
33 of scatter is that the density of fresh-fallen snow decreases with falling temperature.
34 Accordingly, we find in the cold air temperature regime ($T_{air} \leq -25$ °C) a larger ΔT in early



11

1 winter (November-December) when the snow pack is composed of thin, low density fresh
2 snow (and depth hoar) than in late winter (January-February) (SI Fig. 2). Under warm
3 conditions ($-15\text{ °C} < T_{air} \leq -5\text{ °C}$) such a separation is not observed.

4

5 Our analysis (Fig. 1) indicates that some models (CLM4.5, CoLM, JULES) are better able to
6 replicate the observed effect of air temperature on the $\Delta T / d_{snow}$ relationship than others (LPJ-
7 GUESS, MIROC-ESM, ORCHIDEE, UW-VIC). The latter do not fully replicate the larger
8 ΔT under cold air temperature conditions. CLM4.5, CoLM and JULES capture a larger ΔT for
9 colder air temperatures for a given d_{snow} in agreement with the observations. However, for
10 shallow snow JULES simulates twice as large increase of ΔT with increasing d_{snow} for all
11 temperature ranges, compared with observations. Two models (ISBA, UVic) clearly fail in
12 this evaluation. Poor model performance in reflecting air temperature influence on the ΔT
13 $/d_{snow}$ also manifests itself in regime separation of the PDFs (Fig. 2). Some models do not
14 separate the ΔT regimes under different air temperature conditions well or at all (ISBA, LPJ-
15 GUESS, MIROC-ESM, UVic), while others cannot capture the observed cold temperature
16 regime features (i.e., too broad PDFs and shifts towards smaller modal values; ORCHIDEE,
17 UW-VIC). The three models with reasonable inter-variable relations (CLM4.5, CoLM,
18 JULES) also capture the regime separation in the PDFs. These three models as well as LPJ-
19 GUESS and ORCHIDEE also represent the observed greater insulation of early winter snow
20 packs under cold conditions (SI Fig. 2).

21

22 The maps of the $\Delta T / d_{snow}$ correlations in winter (Fig. 3) demonstrate the strong spatial
23 variability in the $\Delta T / d_{snow}$ relationship, but indicate that most models agree on the general
24 large-scale pattern. Some models (CLM4.5, CoLM, ORCHIDEE, UW-VIC) show a
25 reasonable pattern correlation coefficient ($r \geq 0.4$) with observations, while the others do not.
26 Most models simulate the highest positive correlation in the region of the East Siberian Plain
27 and Siberian High lands. In some regions, namely in Scandinavia, West Russian Arctic, West
28 and Central Siberian Plains, the correlation is much weaker and often not statistically
29 significant. These are the regions of large winter snow depth (Sect. 4.1.2) which are
30 influenced by North Atlantic cyclonic activity which brings relatively warm moist air and
31 heavy precipitation in winter (and a positive correlation between snow depth and air
32 temperature), leading to relatively small mean ΔT . Obvious outliers in the $\Delta T / d_{snow}$ correlation
33 map are the LPJ-GUESS and UVic models, which do not reproduce the observed pattern of
34 correlation. UVic calculates a reverse pattern correlation than observations for many regions



12

1 (e.g. significant positive correlation in West Siberian Plain and Central Siberian Highlands).
2 LPJ-GUESS produces very few statistically significant correlations. The model correlations
3 are likely highly sensitive to the quality of the snowfall forcing data, which is uncertain across
4 much of the region due to limited station data that go into most global snowfall products
5 (Hancock et al., 2014; Drobot et al., 2006).

6 **3.2 Variability of soil temperature with air temperature and snow depth**

7 Next we assess whether or not the models can correctly reproduce the interannual near-
8 surface soil temperature (T_{soil}) variability in relation to snow depth (d_{snow}) and near-surface air
9 temperature (T_{air}) variability. Previous authors (Smith and Riseborough, 2002; Sokratov and
10 Barry, 2002; Zhang, 2005; Lawrence and Slater, 2010) have noted that the strength of
11 relationship between T_{soil} and T_{air} is modulated by d_{snow} and the snow insulation effect
12 increases only up to a limiting depth beyond which extra snow makes little difference to soil
13 temperatures. Zhang (2005) reports that the limiting snow depth is approximately 40 cm.

14

15 To inspect the difference of the insulation effects on both sides of such a limiting snow depth,
16 we investigate the T_{soil}/T_{air} relationship under shallow ($d_{snow} \leq 20$ cm) and thick ($d_{snow} \geq 45$ cm)
17 snow conditions. Observations showed that the slope of this relationship is higher when the
18 snow cover is thin, compared with thicker snow conditions (e.g., for Yukon Territory in
19 Canada; Karunaratne and Burn, 2003). Indeed, the Russian observations (Fig. 4, Table 2)
20 indicate a three times stronger T_{soil}/T_{air} relationship (0.62 °C/°C, $R^2=0.8$) under shallow snow
21 pack than thicker snow conditions (0.21 °C/°C, $R^2=0.4$). The average d_{snow} in the shallow snow
22 regime is 13.7 cm and that for the thick snow regime is 58.5 cm, so we would expect, if near-
23 surface air temperature and conductivities were equal in both snow depth classes, a ratio of
24 4.3 in the slopes of Fig. 4. The models that better reproduce the observed $\Delta T / d_{snow}$
25 relationship (CLM4.5, CoLM, JULES) reproduce the observed variation in the T_{soil} / T_{air}
26 relation better than others. JULES and CoLM indicate a factor of 4 change, while CLM4.5
27 indicates a factor of 2 change. Other models (LPJ-GUESS, MIROC-ESM, ORCHIDEE)
28 strongly underestimate the increase of the slope for decreasing snow depth (they simulate a
29 factor change of about 1.5). The two models that had unrealistic $\Delta T / d_{snow}$ relationships (ISBA,
30 UVic) also fail in this evaluation of their T_{soil} / T_{air} relationship. They simulate too strong T_{soil}
31 $/ T_{air}$ relationships (gradients larger than 0.9 °C/°C, $R^2 > 0.7$; Table 2) that are almost completely
32 independent of the snow depth regimes, particularly in ISBA, which is not consistent with
33 observations. These models' spatial correlation patterns between T_{soil} and T_{air} also differ
34 greatly from the observations and the other models (SI Fig. 3) and show very high positive



13

1 correlation ($r > 0.8$) in most regions, as may be expected from the strong relationship shown
2 in Fig. 4. The RMSE of their modeled T_{soil}/T_{air} relationships from observations reaches ca.
3 $10\text{ }^{\circ}\text{C}$.

4
5 The T_{soil}/d_{snow} relationship (Fig. 5) displays the variation of T_{soil} with changing snow depth
6 and emphasizes the weakening role of snow depth for T_{soil} under thick snow conditions. With
7 increasing d_{snow} , soil temperatures asymptotically converge towards a value of around $0\text{ }^{\circ}\text{C}$.
8 Overall, the Russian observations indicate that snow depth above about 80-90 cm has very
9 little additional insulation effect on T_{soil} . Most of the models show consistent results with
10 regard to this aspect, although the inter-quartile range of T_{soil} for a certain snow depth is quite
11 large in some models (ISBA, ORCHIDEE, UVic, UW-VIC) (Fig. 5). The figure further points
12 to the air temperature dependency of the relation. On average, for a given d_{snow} , a colder T_{soil}
13 is observed for colder near-surface air temperatures, compared with warmer air temperatures.
14 Most models can replicate this effect of T_{air} on the T_{soil}/d_{snow} relationship, though with
15 differing accuracy. The RMSE between the observed and modeled relationships can reach ca.
16 $10\text{ }^{\circ}\text{C}$ and more (in ISBA, UVic, UW-VIC), particularly under cold conditions.

17

18 The spatial patterns of the correlation coefficients between T_{soil} and T_{air} (SI Fig. 3) and
19 between T_{soil} and d_{snow} (SI Fig. 4) show a relatively large across-model scatter in the specific
20 regions. Obvious outliers in the T_{soil}/T_{air} correlation maps (SI Fig. 3) are ISBA and UVic
21 which strongly overestimate the correlation ($r > 0.9$) over most of the Arctic. Other models
22 (LPJ-GUESS, ORCHIDEE, UW-VIC) also overestimate the correlation in some regions (e.g.
23 western Russian Arctic, $r > 0.7$). Most of the simulated maps of T_{soil}/d_{snow} correlation (SI Fig.
24 4) agree with the observations on a strong positive correlation in East Siberia. This is a region
25 of relatively shallow snow (10-40 cm; Fig. 6) and there T_{soil} is very sensitive to variations in
26 snow depth (e.g., Romanovsky et al., 2007). Comparing both simulated correlation maps, it is
27 obvious that in this region, T_{soil} correlates more strongly with d_{snow} than with T_{air} , in agreement
28 with the Russian data and earlier studies (Romanovsky et al., 2007; Sherstyukov, 2008).

29 **4 Roles of atmospheric forcing and model processes**

30 The across-model differences in the snow insulation effect, presented by the air temperature -
31 snow depth - soil temperature relationships described above, are partially due to differences in
32 the atmospheric forcing data and also due to differences in the snow and soil physics used in
33 the LSMs. However, because the climate forcing data sets utilized with each model are



14

1 observation-based (except for MIROC-ESM), obvious outliers in individual model
2 performance likely mainly indicate poor or deficient physical descriptions of the air/snow/soil
3 relations in that specific LSM.

4 **4.1 Atmospheric forcing and snow depth**

5 **4.1.1 Air temperature and precipitation**

6 Both near-surface air temperature and precipitation are given by the climate forcing data sets
7 (SI Table 1) for all models, except for MIROC-ESM which simulates both. The across-model
8 differences in forcing air temperature used are relatively small and the simulated spatial
9 patterns of temperature are very similar (SI Fig. 5). All forcing datasets are somewhat colder
10 than Russian station data in their grid cells. The biases range from -0.8 K to -4.7 K (SI Table
11 2), reflecting biases in the climate forcing data used by the models. In contrast, MIROC-ESM
12 has a positive (mean) air temperatures bias of +2.7 K.

13

14 The large-scale patterns of precipitation are similar across the models, but regional differences
15 can be large (SI Fig. 6). The individual differences in precipitation range from -0.2 mm/day
16 to +0.5 mm/day (SI Table 2) relative to the average of the Russian station data. Unfortunately,
17 snowfall was archived in only a few models, however large-scale spatial patterns are similar
18 across these models (SI Fig. 7).

19 **4.1.2 Snow depth**

20 The broad-scale spatial snow depth (d_{snow}) patterns are similar across the models and show
21 general agreement with the observed patterns (Fig. 6). The well-pronounced areas of
22 maximum winter d_{snow} (50-100 cm) are in Scandinavia, the Urals, the West Siberian Plain,
23 Central Siberian Highlands, the Far East, Alaskan Rocky mountains, and Labrador Peninsula
24 and isle of Newfoundland. However, large regional across-model variability is obvious. Some
25 models (JULES, LPJ-GUESS, ORCHIDEE, UVic) underestimate d_{snow} , while others
26 (CLM4.5, CoLM, ISBA, UW-VIC) overestimate it (Fig. 6; SI Table 3). The model biases are
27 quite similar with respect to station observations and GlobSnow data. The evaluation of the
28 model performance for SWE compared to GlobSnow indicates the same bias characteristics
29 as described here for snow depth (not shown). It should be noted, that the models do not
30 account for snowdrift. However, redistribution of snow due to wind is an important aspect,
31 which makes comparison between in-situ measured and modeled snow depths difficult (e.g.,
32 Vionnet et al., 2013; Sturm and Stuefer, 2013; Gispnas et al., 2014).



15

1

2 Precipitation/snowfall across-model differences cannot be the primary explanation of these
3 d_{snow} differences since some models (JULES, MIROC-ESM, ORCHIDEE) have positive bias
4 in precipitation (> 0.2 mm/d, SI Table 2) but simulate much lower d_{snow} compared to other
5 models (Fig. 6, SI Figs. 6, 7, SI Table 3). Across-model differences in the interannual
6 variability of winter precipitation do not translate simply to corresponding differences in the
7 interannual d_{snow} variability (not shown). For example, UVic calculates the (unrealistically)
8 largest interannual d_{snow} variability in the boreal Europe permafrost region which is not
9 reflected in the precipitation variability. These results indicate that the simulated snow depth
10 is a function of both, the prescribed winter precipitation, and the model's snow energy and
11 water balance.

12 4.2 Model processes

13 We have shown that the across-model spread in the representation of snow insulation effects
14 (Sects. 3.1, 3.2) can not predominantly be explained by differences in the forcing data (Sect.
15 4.1), but to a large extent is due to the representation of snow processes in the models. By
16 considering the relationship plots and the conditional PDFs (Figs. 1, 2, 4, and 5) we were
17 able to sort the models in terms of their snow insulation performance. In this section we
18 discuss the influence of the different snow parameterizations in the models.

19

20 Models with better performance (CLM4.5, CoLM, JULES) apply multi-layer snow schemes.
21 This allows them to simulate more realistic (stronger) insulation because they consider the
22 snowpack's vertical structure and variability. They calculate the energy and mass balance in
23 each snow layer, are able to capture nonlinear profiles of snow temperature, and can also
24 account for thermal insulation within the snowpack such as when the upper layer thermally
25 insulates the lower layers (e.g., Dutra et al., 2012). These models also incorporate storage and
26 refreezing of liquid water within the snow, parameterize wet snow metamorphism, snow
27 compaction, and snow thermal conductivity (Table 1), which have been found to be among
28 the most important processes for good snow depth and surface soil temperature simulation
29 (e.g., Wang et al., 2013).

30

31 An underestimated snow depth directly leads to insulation that is too weak in JULES, LPJ-
32 GUESS, ORCHIDEE, and UVic (Fig. 6, SI Table 3). However only in ORCHIDEE and UVic
33 does this lead to a significant underestimation of ΔT (SI Table 3, SI Fig. 8) indicating bias



16

1 compensation in the two other models. Thus, compensating error effects occur due to snow
2 density and conductivity (SI Fig. 9, Table 1), which impact snow thermal insulation.

3

4 Our analysis showed that two models (ISBA, UVic) have T_{soil}/T_{air} correlation that are too
5 high indicating that they do not represent the modulation of the T_{soil}/T_{air} relationship by snow
6 depth (Fig. 4). This is consistent with their underestimation of ΔT (Figs. 1 and 2, SI Fig. 8, SI
7 Table 3). In UVic, the snowpack is treated not as a separate layer but as an extension of the
8 top soil layer and a combined surface-to-soil thermal conductivity is calculated (Table 1).
9 Such a scheme largely negates or reduces the insulating capacity of snow (Slater et al., 2001).
10 Koven et al. (2013) noted that such a scheme simulates very little warming of soil, and
11 sometimes even cooling. The slightly underestimated snow depth (SI Table 3, Fig. 6)
12 contributes (but not as the primary factor) to reduced snow insulation, as reported for UVic
13 (Avis, 2012).

14

15 ISBA strongly underestimates ΔT , while strongly overestimating d_{snow} , compared with
16 observations (SI Table 3, Fig. 6). However, ISBA uses the same atmospheric forcing data as
17 JULES (accordingly the air temperature and precipitation are quite similar; SI Table 2). Also,
18 the model's snow density ($150\text{-}250\text{ kg m}^{-3}$) is similar to other models (CLM45, CoLM,
19 JULES) (SI Fig. 9) and in agreement with Zhong et al. (2013) who report snow density values
20 of on $180\text{-}250\text{ kg m}^{-3}$ for tundra/taiga and $156\text{-}193\text{ kg m}^{-3}$ for alpine snow classes in winter.
21 This apparent contradiction comes from the parameterization of snow cover fraction within
22 each grid cell (SCF). The version of ISBA used here calculates a unique superficial soil
23 temperature whether or not the soil is covered by snow and all the energy and radiative fluxes
24 are area-weighted by SCF (equations 7 and 20 in *Douville et al.*, 1995). In order to get
25 reasonable albedos in snow-covered forests, as is necessary when ISBA is coupled to the
26 CNRM-CM climate model, the parameterization gives very low SCF in the boreal forest
27 (between 0.2 and 0.5). Hence, snow insulates only 20% to 50% of the grid cell, despite fairly
28 high snow depths. The heat fluxes from the snow-covered fraction are averaged with the
29 fluxes from the snow-free surface, strongly concealing the actual insulating effect of snow
30 and underestimating it over the grid cell. Using the detailed snow model Crocus (Brun et al.,
31 1992; Vionnet et al., 2012) with a SCF equal to 100% leads to an almost perfect simulation of
32 near-surface soil temperature over Northern Eurasia (Brun et al., 2013). A similar experiment
33 with ISBA and a SCF equal to 100% (Decharme et al., 2015) leads to good performances
34 showing that the low ΔT in ISBA despite high snow depth in the present study is mostly due



17

1 to this sub-grid snow fraction. The results are further improved by updating the snow albedo
2 and snow densification parameterization.

3

4 Interestingly, the ORCHIDEE performance in simulating snow depth and ΔT is similar to
5 UVic (underestimation of d_{snow} and ΔT ; SI Table 3). However, ORCHIDEE can better
6 represent the observed T_{soil}/T_{air} relationship and its modulation due to snow pack.
7 ORCHIDEE employs, similarly to UVic, a fixed snow density and thermal conductivity.
8 However, in contrast with UVic, ORCHIDEE applies a multi-layer scheme and simulates heat
9 diffusion in the snowpack in up to 7 discrete layers (Table 1; Koven et al., 2009). This helps
10 resolving the snow thermal gradients between the top and the base of the snow cover, and
11 might explain how some of the snow insulation effects are reasonably represented in
12 ORCHIDEE, despite the simpler treatment of temperature diffusion.

13 5 Summary and conclusions

14 The aim of this work was to evaluate how state-of-the-art LSMs capture the observed
15 relationship between winter near-surface soil and air temperatures (T_{soil} , T_{air}) and their
16 modulation by snow depth (d_{snow}) and climate regime. We presented some benchmarks to
17 evaluate model performance. The results are based on the comparison of LSMs with a novel
18 comprehensive Russian station data set.

19

20 We see large differences across the models in their mean air-soil temperature difference (ΔT)
21 of 3 to 14 K, in the gradient between near-surface soil and air temperatures (T_{soil}/T_{air}) (0.49 to
22 0.96 °C/°C for shallow snow, 0.13 to 0.93 °C/°C for thick snow), and in the increase of ΔT
23 with increasing snow depth (modal value of ΔT PDF: 0 to 10 K for shallow snow, 5 to 21 K
24 for thick snow). Most of the nine models compare to the observations reasonably well
25 (observations: $\Delta T = 12$ K, modal ΔT values of 5 K for shallow snow and of 14 K for thick
26 snow, $T_{soil}/T_{air} = 0.62$ °C/°C for shallow snow, $T_{soil}/T_{air} = 0.21$ °C/°C for thick snow). Several
27 models also capture the modulation by air temperature condition (larger increase in ΔT with
28 increasing d_{snow} under colder conditions) and display the control of snow depth on T_{soil}
29 (weaker T_{soil}/T_{air} relationship under thicker snow). However, while they generally capture
30 these observed relationships, their strength can differ in the individual models. Two models
31 (ISBA, UVic) show the largest deficits in snow insulation effects and cannot separate the ΔT
32 regimes neither for different snow depths nor for different air temperature conditions.

33



18

1 The primary aim of this study was to use this ensemble of models to document model
2 performance with respect to T_{soil} versus T_{air} relationships, and to identify those with better
3 performance, rather than to quantify the best model. We were able to attribute performance
4 strength/weakness to snow model features and complexity. Models with better performance
5 apply multi-layer snow schemes and consider complex snow processes (e.g. storage and
6 refreezing of liquid water within the snow, wet snow metamorphism, snow compaction).
7 Those models which show limited skill in snow insulation representation (underestimated ΔT ,
8 very weak dependency of ΔT on d_{snow} , almost unity ratio of T_{soil}/T_{air}) have some deficiencies
9 in the simulation of heat transfer in snow and soil layer, particularly in the representation of
10 snow depth and density (conductivity). We also emphasize that compensating errors in snow
11 depth and conductivity can occur. For example, an excessive correlation between T_{soil} and T_{air}
12 can be attributed to excessively high thermal conductivity even when the snow depth is
13 correctly (or over) simulated. This finding underscores the need for detailed model
14 evaluations using multiple, independent performance metrics to establish that the models get
15 the right functionality for the right reason. It should be noted that the treatment of ground
16 properties, particularly soil organic matter and soil moisture/ice content, also affect the
17 simulated winter ground temperatures. The specific evaluation of these individual processes is
18 more robustly investigated with experiments conducted for individual models (e.g. recently,
19 Wang et al., 2013; Gubler et al., 2013; Decharme et al., 2015).

20

21 A realistic simulation of the snow is a key pre-requisite for accurate modeling of the soil
22 thermal dynamics across the permafrost region. The areal cover of Northern Hemisphere near-
23 surface permafrost varies greatly across the nine models in the hindcast simulation (1960-
24 2009). Some of the better performing snow insulation effect models (CLM4.5, JULES)
25 simulate a near-surface permafrost area of 12 to 16 million km², which is comparable with the
26 IPA map estimate (16 million km²) (Brown et al., 1997; Slater and Lawrence, 2013). CoLM
27 and ORCHIDEE, identified as reasonable models with respect to snow insulation, simulate
28 much lower (7 million km²) and higher (20 million km²) areas, respectively. However, ISBA,
29 one of the two models that showed rather limited skill in representing snow insulation effects,
30 also simulates the highest permafrost area (20 million km²). This is consistent with previous
31 studies (e.g., Vavrus, 2007; Koven et al., 2013) which concluded that first-order control on
32 modeled near-surface permafrost distribution is the representation of the air-to-surface soil
33 temperature difference. When the models with poor snow models are eliminated, there is no
34 clear relationship between the quality of the snow insulation in the models and the simulated



19

1 area of permafrost, likely because several other factors such as differences in the treatment of
2 soil organic matter, soil hydrology, surface energy calculations, model soil column depth, and
3 vegetation also provide important controls on simulated permafrost distribution (Marchenko
4 and Etzelmüller, 2013).

5

6 *Acknowledgments.* The data will be made available through the National Snow and Ice Data
7 Center (NSIDC; <http://nsidc.org>); the contact person is Kevin Schaefer
8 (kevin.schaefer@nsidc.org). This study was supported by the Permafrost Carbon
9 Vulnerability Research Coordination Network, which is funded by the U.S. National Science
10 Foundation (NSF). Any use of trade, firm, or product names is for descriptive purposes only
11 and does not imply endorsement by the U.S. Government. E.J.B. was supported by the Joint
12 UK DECC / Defra Met Office Hadley Centre Climate Program (GA01101). E.J.B., S.P., P.C.
13 and G.K. were supported by the European Union Seventh Framework Program (FP7/2007-
14 2013) under grant agreement n°282700. T.J.B. was supported by grant 1216037 from the NSF
15 Science, Engineering and Education for Sustainability (SEES) Post-Doctoral Fellowship
16 program. This research was sponsored by the Integrated approaches and impacts, China
17 Global Change Program (973 Project), National Basic Research Program of China Grant
18 2015CB953602 and the National Natural Science Foundation of China Grant 40905047.

19 **References**

- 20 Anderson, E.A.: A point energy and mass balance model of a snow cover, Office of
21 Hydrology, National Weather Service, Silver Spring, Maryland, NOAA Technical Report
22 NWS 19, 1976.
- 23 Andreadis, K., Storck, P. and Lettenmaier, D.P.: Modeling snow accumulation and ablation
24 processes in forested environments, *Water Resour. Res.*, 45, W05429,
25 doi:10.1029/2008WR007042, 2009.
- 26 Avis, C.A.: Simulating the present-day and future distribution of permafrost in the UVic Earth
27 System Climate Model, Dissertation, University of Victoria, Canada, 274pp, 2012.
- 28 Bartlett, P.A., MacKay, M.D., Verseghy, D.L.: Modified snow algorithms in the Canadian
29 Land Surface Scheme: model runs and sensitivity analysis at three boreal forest stands,
30 *Atmosphere-Ocean*, 44, 207–222, 2006.
- 31 Best, M.J., and 16 co-authors: The Joint UK Land Environment Simulator (JULES), model
32 description—Part 1: energy and water fluxes, *Geosci. Model. Dev.*, 4, 677–699,
33 doi:10.5194/gmd-4-677-2011, 2011.



20

- 1 Boone, A., and Etchevers, P.: An intercomparison of three snow schemes of varying
2 complexity coupled to the same land-surface model: Local scale evaluation at an Alpine
3 site, *J. Hydrometeor.*, 2, 374-394, 2001.
- 4 Brown, J., Ferrians, O.J., Heginbottom, J.A. and Melnikov, S.E.: International Permafrost
5 Association Circum-Arctic Map of Permafrost and Ground Ice Conditions, scale
6 1:10,000,000, Circum-Pacific Map Series, USGS Circum-Pacific Map Series, Map CP-45,
7 1997.
- 8 Brun, E., David, P., Sudul, M. and Brunot, G.: A numerical model to simulate snow cover
9 stratigraphy for operational avalanche forecasting, *J. Glaciol.*, 38, 13–22, 1992.
- 10 Brun, E., Vionnet, V., Boone, A., Decharme, B., Peings, Y., Valette, R., Karbou, F. and
11 Morin, S.: Simulation of northern Eurasian local snow depth, mass and density using a
12 detailed snowpack model and meteorological reanalysis, *J. Hydrometeorol.*, 14, 203–214,
13 doi:10.1175/jhm-d-12-012.1, 2013.
- 14 Cook, B.I., Bonan, G.B., Levis, S. and Epstein, H.E.: The thermoinsulation effect of snow
15 cover within a climate model, *Clim. Dyn.*, 31, 107-124, doi:10.1007/s00382-007-0341-y,
16 2008.
- 17 Dai, Y., Zeng, X., Dickinson, R.E., Baker, I., Bonan, G.B., Bosilovich, M.G., Denning, A.S.,
18 Dirmeyer, P.A., Houser, P.R., Niu, G., Oleson, K.W., Schlosser, C.A. and Yang, Z.: The
19 Common Land Model (CLM), *Bull. Am. Meteorol. Soc.*, 84, 1013–1023,
20 doi:10.1175/BAMS-84-8-1013, 2003.
- 21 Dankers, R., Burke, E.J., and Price, J.: Simulation of permafrost and seasonal thaw depth in
22 the JULES land surface scheme, *The Cryosphere*, 5, 773-790, doi:10.5194/tc-5-773-2011,
23 2011.
- 24 Decharme, B., Brun, E., Boone, A., Delire, C., Le Moigne, P. and Morin, S.: Impacts of snow
25 and organic soils parameterization on North-Eurasian soil temperature profiles simulated
26 by the ISBA land surface model, *The Cryosphere Discussions*, 9, 6733-6790,
27 doi:10.5194/tcd-9-6733-2015, 2015.
- 28 Douville, H., Royer, J.-F. and Mahfouf, J.-F.: A new snow parameterization for the Meteo-
29 France climate model. Part 1: Validation in stand-alone experiments, *Clim. Dyn.*, 12, 21–
30 35, 1995.
- 31 Drobot, S., Maslanik, J., Herzfeld, U.C., Fowler, C. and Wu, W.: Uncertainty in temperature
32 and precipitation datasets over terrestrial regions of the Western Arctic, *Earth Interactions*,
33 10 (23), 1-17, 2006.



21

- 1 Dutra, E., Viterbo, P., Miranda, P.M.A. and Balsamo, G.: Complexity of snow schemes in a
2 climate model and its impact on surface energy and hydrology, *J. Hydrometeorol.*, 13,
3 521–538, doi:10.1175/jhm-d-11-072.1, 2012.
- 4 Dutra, E., Balsamo, G., Viterbo, P., Miranda, P.M.A., Beljaars, A., Schär, C. and Elder, K.:
5 An improved snow scheme for the ECMWF land surface model: description and offline
6 validation, *J. Hydrometeorol.*, 11, 899-916, 2010.
- 7 Essery, R., Morin, S., Lejeune, Y. and Ménard, C.B.: A comparison of 1701 snow models
8 using observations from an alpine site, *Adv. Water Resour.*, 55, 131–148,
9 doi:10.1016/j.advwatres.2012.07.013, 2013.
- 10 Essery, R.L.H., Rutter, N., Pomeroy, J., Baxter, R., Staehli, M., Gustafsson, D., Barr, A.,
11 Bartlett, P. and Elder, K.: SnowMIP2: An evaluation of forest snow process simulations,
12 *Bull. Am. Meteorol. Soc.*, 90, 1120-1135, doi:10.1175/2009BAMS2629.1, 2009.
- 13 Ge, Y. and Gong, G.: Land surface insulation response to snow depth variability, *J. Geophys.*
14 *Res.*, 115, D08107, doi:10.1029/2009JD012798, 2010.
- 15 Gerten, D., Schaphoff, S., Haberlandt, U., Lucht, W. and Sitch, S.: Terrestrial vegetation and
16 water balance: Hydrological evaluation of a dynamic global vegetation model, *J. Hydrol.*,
17 286, 249–270, 2004.
- 18 Gispnas, K., Westermann, S., Schuler, T., Litherland, T., Isaksen, K., Boike, J. and Etzelmüller,
19 B.: A statistical approach to represent small-scale variability of permafrost temperatures
20 due to snow cover, *The Cryosphere*, 8, 2063-2074, doi: 10.5194/tc-8-2063-2014, 2014.
- 21 Gouttevin, I., Menegoz, M., Domine, F., Krinner, G., Koven, C.D., Ciais, P., Tarnocai, C. and
22 Boike, J.: How the insulating properties of snow affect soil carbon distribution in the
23 continental pan-Arctic area, *J. Geophys. Res.*, 117, G02020, doi:10.1029/2011JG001916,
24 2012.
- 25 Gubler, S., Endrizzi, S., Gruber, S. and Purves, R.S.: Sensitivities and uncertainties of
26 modeled ground temperatures in mountain environments, *Geosci. Model Dev.*, 6, 1319-
27 1336, doi:10.5194/gmd-6-1319-2013, 2013.
- 28 Hancock, S., Huntley, B., Ellis, R. and Baxter, R.: Biases in reanalysis snowfall found by
29 comparing the Jules land surface model to GlobSnow, *J. Clim.*, 27(2), 624-632, 2014.
- 30 Jafarov, E.E., Nicolsky, D.J., Romanovsky, V.E., Walsh, J.E., Panda, S.K. and Serreze, M.C.:
31 The effect of snow: How to better model ground surface temperatures, *Cold Regions Sci.*
32 *Technol.*, 102, 63-77, doi:10.1016/j.coldregions.2014.02.007, 2014.



22

- 1 Ji, D., Wang, L., Feng, J., Wu, Q., Cheng, H., et al.: Description and basic evaluation of
2 Beijing Normal University Earth System Model (BNU-ESM) version 1, *Geosci. Model*
3 *Dev.*, 7, 2039–2064, 2014.
- 4 Jordan, R.: A one-dimensional temperature model for a snow cover, technical documentation
5 for SNTHERM.89, Special Report 91-16, U.S. Army Cold Regions Research and
6 Engineering Laboratory, Hanover, N.H, 1991.
- 7 Karunaratne, K.C., and Burn, C.R.: Freezing n-factors in discontinuous permafrost terrain,
8 Takhini River, Yukon Territory, Canada Proc. 8th Int. Conf. on Permafrost, Zurich, Eds. M.
9 Phillips, S.M. Springman and L.U.Arenson, pp 519–24, 2003.
- 10 Koven, C.D., Riley, W.J. and Stern, A.: Analysis of Permafrost Thermal Dynamics and
11 Response to Climate Change in the CMIP5 Earth System Models, *J. Clim.*, 26, 1877–1900.
12 doi:10.1175/JCLI-D-12-00228.1, 2013.
- 13 Koven, C., Friedlingstein, P., Ciais, P., Khvorostyanov, D., Krinner, G. and Tarnocai, C.: On
14 the formation of high-latitude soil carbon stocks: Effects of cryoturbation and insulation by
15 organic matter in a land surface model, *Geophys. Res. Lett.*, 36, L21501,
16 doi:10.1029/2009GL040150, 2009.
- 17 Lawrence, D.M., and Slater, A.G.: The contribution of snow condition trends to future ground
18 climate, *Clim. Dyn.*, 34, 969–981, doi:10.1007/s00382-009-0537-4, 2010.
- 19 Ling, F., and Zhang, T.: Sensitivity study of tundra snow density on surface energy fluxes and
20 ground thermal regime in Northernmost Alaska, *Cold Regions Sci. Technol.*, 44, 121–130,
21 2006.
- 22 Marchenko, S. and Etzelmueller, B.: Permafrost: Formation and Distribution, Thermal and
23 Mechanical Properties. In: John F. Shroder (ed.) *Treatise on Geomorphology*, Volume 8,
24 pp. 202–222. San Diego: Academic Press, 2013.
- 25 Meissner, K.J., Weaver, A.J., Matthews, H.D. and Cox, P.M.: The role of land-surface
26 dynamics in glacial inception: A study with the UVic earth system model, *Clim. Dyn.*, 21,
27 515–537, 2003.
- 28 Morse, P.D., Burn, C.R., and Kokelj, S.V.: Influence of snow on near-surface ground
29 temperatures in upland and alluvial environments of the outer Mackenzie Delta, Northwest
30 Territories, *Can. J. Earth Sci.*, 49, 895–913, doi:10.1139/E2012-012, 2012.
- 31 Muskett, R.: Remote sensing, model-derived and ground measurements of snow water
32 equivalent and snow density in Alaska, *Int. J. Geosci.*, 3, 1127–1136,
33 doi:10.4236/ijg.2012.35114, 2012.



23

- 1 Nicolsky, D.J., Romanovsky, V.E., Alexeev, V.A. and Lawrence, D.M.: Improved modelling
2 of permafrost dynamics in a GCM land-surface scheme, *Geophys. Res. Lett.*, 34, L08501,
3 doi:10.1029/2007GL029525, 2007.
- 4 Oleson, K.W., Lawrence, D.M., Bonan, G.B., Drewniak, B., Huang, M., Koven, C.D., Levis,
5 S., Li, F., Riley, W.J., Subin, Z.M., Swenson, S.C., Thornton, P.E., Bozbiyik, A., Fisher,
6 R., Kluzek, E., Lamarque, J.-F., Lawrence, P.J., Leung, L.R., Lipscomb, W., Muszala, S.,
7 Ricciuto, D.M., Sacks, W., Sun, Y., Tang, J., Yang, Z.-L.: Technical description of version
8 4.5 of the Community Land Model (CLM). NCAR Technical Note NCAR/TN-503+STR,
9 doi: 10.5065/D6RR1W7M, 2013.
- 10 Paquin, J.-P., and Sushama, L.: On the Arctic near-surface permafrost and climate
11 sensitivities to soil and snow model formulations in climate models, *Clim. Dyn.*, 44, 203-
12 228, doi:10.1007/s00382-014-2185-6, 2015.
- 13 Park, H., Fedorov, A.N., Zheleznyak, M.N., Konstantinov, P.Y. and Walsh, J.E.: Effect of
14 snow cover on pan-Arctic permafrost thermal regimes, *Clim. Dyn.*, 44, 2873-2895,
15 doi:10.1007/s00382-014-2356-5, 2015.
- 16 Peng, S., Ciais, P., Krinner, G., Wang, T., Gouttevin, I., McGuire, A., Lawrence, D., Burke,
17 E., Chen, X., Decharme, B., Koven, C., MacDougall, A., Rinke, A., Saito, K., Zhang, W.,
18 Alkama, R., Bohn, T.J., Delire, C., Hajima, T., Ji, D., Lettenmaier, D.P., Miller, P.A.,
19 Moore, J.C., Smith, B. and Sueyoshi, T.: Simulated high-latitude soil thermal dynamics
20 during the past four decades, *The Cryosphere*, 10, 1–14, doi:10.5194/tc-10-1-2016, 2015.
- 21 Rawlins, M., McGuire, A., Kimball, J., Dass, P., Lawrence, D., Burke, E., Chen, X., Delire,
22 C., Koven, C., MacDougall, A., Peng, S., Rinke, A., Saito, K., Zhang, W., Alkama, R.,
23 Bohn, T.J., Ciais, P., Decharme, B., Gouttevin, I., Hajima, T., Ji, D., Krinner, G.,
24 Lettenmaier, D.P., Miller, P.A., Moore, J.C., Smith, B. and Sueyoshi, T.: Assessment of
25 model estimates of land–atmosphere CO₂ exchange across Northern Eurasia,
26 *Biogeosciences*, 12, 4385-4405, doi:10.5194/bg-12-4385-2015, 2015.
- 27 Riseborough, D.W.: An analytical model of the ground surface temperature under snow cover
28 with soil freezing, 58th Eastern Snow Conference, Ottawa, Ontario, Canada, 2001
- 29 Romanovsky, V.E., Sazonova, T.S., Balobaev, V.T., Shender, N.I. and Sergueev, D.O.: Past
30 and recent changes in air and permafrost temperatures in eastern Siberia, *Glob. Planet.*
31 *Change*, 56, 399-413, doi:10.1016/j.gloplacha.2006.07.022, 2007.
- 32 Romanovsky, V.E., and Osterkamp, T.E.: Interannual variations of the thermal regime of the
33 active layer and near-surface permafrost in Northern Alaska, *Permafrost Periglac. Process.*,
34 6, 313–335, 1995.



24

- 1 Saha, S., Rinke, A., Dethloff, K. and Kuhry, P.: Influence of complex land surface scheme on
2 Arctic climate simulations, *J. Geophys. Res.*, 111, D22104, doi:10.1029/2006JD007188,
3 2006.
- 4 Schaefer, K., Zhang, T., Bruhwiler, L. and Barrett, A.P.: Amount and timing of permafrost
5 carbon release in response to climate warming, *Tellus B*, 63, 165–180, doi:10.1111/j.1600-
6 0889.2011.00527.x, 2011.
- 7 Schuur, E.A.G., and 18 coauthors: Vulnerability of permafrost carbon to climate change:
8 Implications for the global carbon cycle, *Bioscience*, 58, 701-714. doi:10.1641/b580807,
9 2008.
- 10 Sherstyukov, A.B.: Correlation of soil temperature with air temperature and snow cover depth
11 in Russia, *Earth's Cryosphere*, 12, 79-87, 2008.
- 12 Singh, V.P., Singh, P. and Haritashya, U.: *Encyclopedia of snow, ice and glaciers*, Springer,
13 1240p, 2011.
- 14 Slater, A.G., Schlosser, C.A. and Desborough, C.E.: The representation of snow in land-
15 surface schemes: Results from PILPS 2(d), *J. Hydrometeorol.*, 2, 7-25, 2001.
- 16 Slater, A., and Lawrence, D.: Diagnosing present and future permafrost from climate models,
17 *J. Clim.*, doi:10.1175/JCLI-D-12-00341.1, 2013.
- 18 Smith, M.W., and Riseborough, D.W.: Climate and the limits of permafrost: a zonal analysis,
19 *Permafrost Periglac. Process.*, 13, 1-15, doi: 10.1002/ppp.410, 2002.
- 20 Sokratov, S.A., and Barry, R.G.: Intraseasonal variation in the thermoinsulation effect of
21 snow cover on soil temperatures and energy balance, *J. Geophys. Res.*, 107,
22 doi:10.1029/2001JD000489, 2002.
- 23 Sturm, M., Holmgren, J., König, M. and Morris, K.: The thermal conductivity of seasonal
24 snow, *J. Glaciol.*, 43 (143), 26–41, 1997.
- 25 Sturm, M., and Stuefer, S.: Wind-blown flux rates derived from drifts at arctic snow fences, *J.*
26 *Glaciol.*, 59 (213), 21-34, 2013.
- 27 Swenson, S.C., and Lawrence, D.M.: A new fractional snow-covered area parameterization
28 for the Community Land Model and its effect on the surface energy balance, *J. Geophys.*
29 *Res.*, 117, D21107, doi:10.1029/2012JD018178, 2012.
- 30 Takala, M., Luojus, K., Pulliainen, J., Derksen, C., Lemmetyinen, J., Karna, J.P., Koskinen, J.
31 and Bojkov, B.: Estimating Northern Hemisphere snow water equivalent for climate
32 research through assimilation of space-borne radiometer data and ground-based
33 measurements, *Remote Sens. Environ.*, 115, 3517-3529, 2011.



25

- 1 Takata, K., Emori, S. and Watanabe, T.: Development of the minimal advanced treatments of
2 surface interaction and runoff, *Glob. Planet. Change*, 38, 209–222, 2003.
- 3 Vavrus, S.J.: The role of terrestrial snow cover in the climate system, *Clim. Dyn.*, 20, 73–88,
4 doi:10.1007/s00382-007-0226-0, 2007.
- 5 Vionnet, V., Brun, E., Morin, S., Boone, A., Faroux, S., Moigne, P.L., Martin, E. and
6 Willemet, J.-M.: The detailed snowpack scheme Crocus and its implementation in
7 SURFEX v7.2, *Geosci. Model Dev.*, 5, 773–791, 2012.
- 8 Vionnet, V., Guyomarch, G., Martin, E., Durand, Y., Bellot, H., Bel, C. and Pugliese, P.:
9 Occurrence of blowing snow events at an alpine site over a 10-year period: observations
10 and modelling, *Adv. Water Resour.*, 55, 53–63, 2013.
- 11 Wang, T., Otle, C., Boone, A., Ciais, P., Brun, E., Morin, S., Krinner, G., Piao, S. and Peng,
12 S.: Evaluation of an improved intermediate complexity snow scheme in the ORCHIDEE
13 land surface model, *J. Geophys. Res.*, 118, 6064–6079, doi:10.1002/jgrd.50395, 2013.
- 14 Wania, R., Ross, I. and Prentice, I.C.: Integrating peatlands and permafrost into a dynamic
15 global vegetation model: 2. Evaluation and sensitivity of vegetation and carbon cycle
16 processes, *Global Biogeochem. Cycles*, 23, GB3015, doi:10.1029/2008GB003413, 2009.
- 17 Zhang, T.: Influence of the seasonal snow cover on the ground thermal regime: An overview,
18 *Rev. Geophys.*, 43, RG4002, doi:10.1029/2004RG000157, 2005.
- 19 Zhang, T., Osterkamp, T.E. and Stamnes, K.: Influence of the depth hoar layer of the seasonal
20 snow cover on the ground thermal regime, *Water Resour. Res.*, 32, 2075–2086,
21 doi:10.1029/96WR00996, 1996.
- 22 Zhong, X., Zhang, T. and Wang, K.: Snow density climatology across the former USSR, *The*
23 *Cryosphere*, 8, 785–799, doi:10.5194/tc-8-785-2014, 2013.

24
25
26
27
28
29
30



26

1 **Tables**

2

3 **Table 1.** PCN snow model details.

Model Reference for snow scheme	Snow scheme ¹	Snow layers	Water phases	Liquid water treatment ²	Snow density ³	Snow thermal conductivity ⁴
CLM4.5 Swenson and Lawrence, 2012 Oleson et al., 2013	ML	Dynamic (max. 5)	Liquid, Ice	Bucket-type prognostic in each layer	depends on snow depth; compaction ^{3) a,b,c}	quadratic equation on ρ
CoLM Dai et al., 2003 Ji et al. 2014	ML	Dynamic (max. 5)	Liquid, Ice	Bucket-type prognostic in each layer	depends on snow depth; compaction ^{3) a,b,c}	quadratic equation on ρ
ISBA Boone and Etchevers, 2001	ML	Static (3)	Liquid, Ice, Vapor	Diagnosed from snow temperature, mass, density	compaction ^{3) a,b}	quadratic equation on ρ , contribution due to vapor transfer
JULES Best et al., 2011	ML	Dynamic (max. 3)	Liquid, Ice, Vapor	Bucket-type prognostic in each layer	compaction ^{3) a}	power equation on ρ
LPJ-GUESS Gerten et al., 2004 Wania et al., 2009	BL	Static (1)	Ice	Not represented	fixed 362 kg m ⁻³	fixed 0.196 Wm ⁻¹ K ⁻¹
MIROC-ESM Takata et al., 2003	ML	Dynamic (max. 3)	Ice	Not represented	fixed 300 kg m ⁻³	fixed 0.3 Wm ⁻¹ K ⁻¹
ORCHIDEE Gouttevin et al., 2012	ML	Dynamic (max. 7)	Ice	Not represented	fixed 330 kg m ⁻³	fixed 0.25 Wm ⁻¹ K ⁻¹ for tundra, 0.042 Wm ⁻¹ K ⁻¹ for taiga
UVic Meissner et al., 2003 Avis, 2012	I	Static (1)	Ice	Not represented	fixed 330 kg m ⁻³	bulk conductivity
UW-VIC Andreadis et al., 2009	BL	Dynamic (max. 2)	Liquid, Ice, Vapor	Constant liquid water holding capacity	compaction ^{3) a,b}	fixed 0.7 Wm ⁻¹ K ⁻¹

4 ¹ ML: Multi-layer, BL: Bulk-layer, I: Implicit; according to Slater et al. (2001)

5 ² Not represented means dry snow

6 ³ Processes for densification of the snow: a) mechanical compaction (due to the weight of the overburden), b)
 7 thermal metamorphosis (via the melting–refreezing process), c) destructive metamorphism (crystal breakdown
 8 due to wind, thermodynamic stress); Anderson (1976), Jordan (1991), Kojima (1967)

9 ⁴ quadratic equation on ρ according to Jordan (1991), Anderson (1976); contribution due to vapor transfer
 10 according to Sun et al.(1999)

11

12



27

1 **Table 2.** Sensitivity of near-surface soil temperature (T_{soil}) to air temperature (T_{air}) in winter
 2 (DJF) calculated by the slopes of the linear regression between T_{soil} (°C) and T_{air} (°C) for
 3 different regimes of snow depth (d_{snow}), using data from all Russian station grid points and 21
 4 individual winter 1980-2000. All relationships are statistically significant at $p \leq 0.01$.

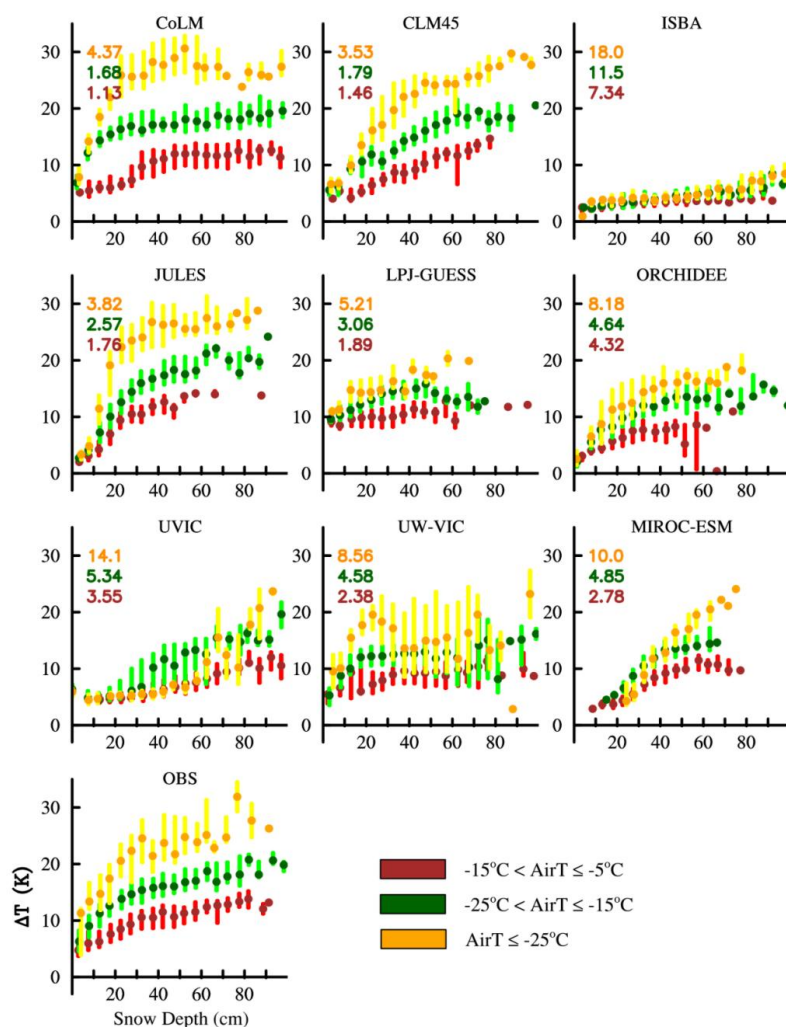
5

	Snow depth regimes			
	Shallow		Thick	
	$d_{snow} \leq 20$ cm		$d_{snow} \geq 45$ cm	
	T_{soil}/T_{air} (°C/°C)	R^2	T_{soil}/T_{air} (°C/°C)	R^2
Observation	0.62	0.79	0.21	0.41
CLM4.5	0.69	0.89	0.33	0.56
CoLM	0.49	0.73	0.13	0.44
ISBA	0.93	0.98	0.93	0.94
JULES	0.68	0.77	0.19	0.46
LPI-GUESS	0.73	0.89	0.52	0.75
MIROC-ESM	0.78	0.98	0.49	0.67
ORCHIDEE	0.86	0.83	0.56	0.64
UVic	0.96	0.97	0.81	0.68
UW-VIC	0.54	0.74	0.76	0.65

6



28



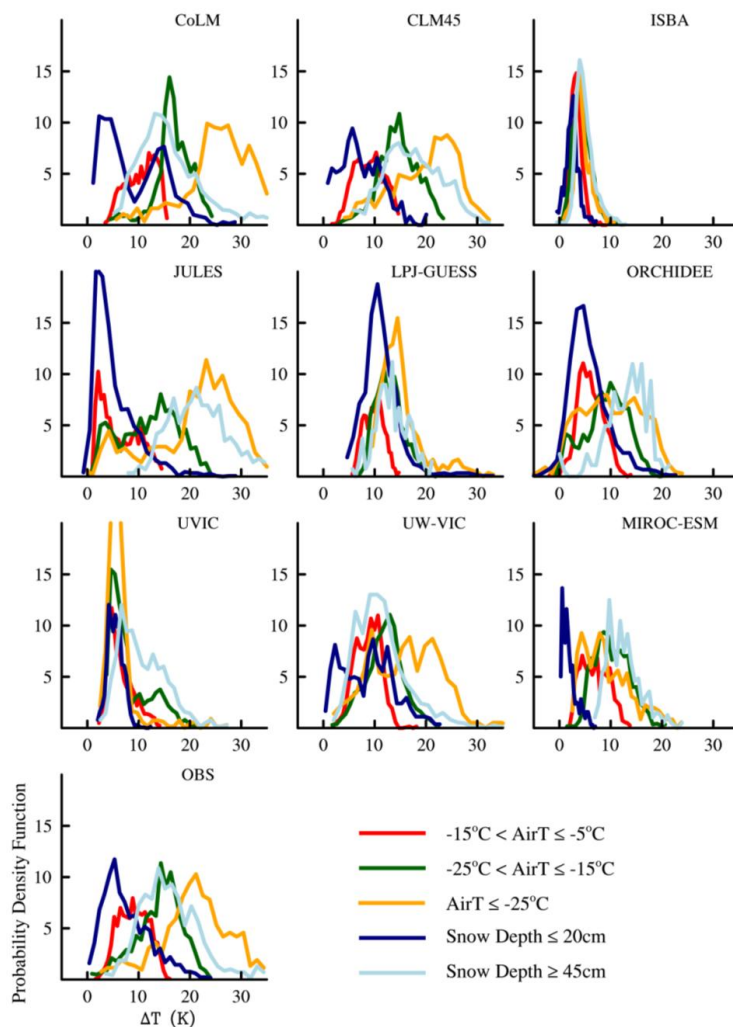
1

2

3 **Figure 1.** Variation of ΔT (K), the difference between soil temperature at 20 cm depth and air
 4 temperature) with snow depth (cm) for winter 1980-2000. The dots represent the medians of 5
 5 cm snow depth bins and the upper and lower bars indicate the 25th and 75th percentiles,
 6 calculated from all Russian station grid points ($n=268$) and 21 individual winters. The
 7 numbers in each model panel indicate the RMSE between the observed and modeled
 8 relationship. Color represents different air temperature regimes.



29

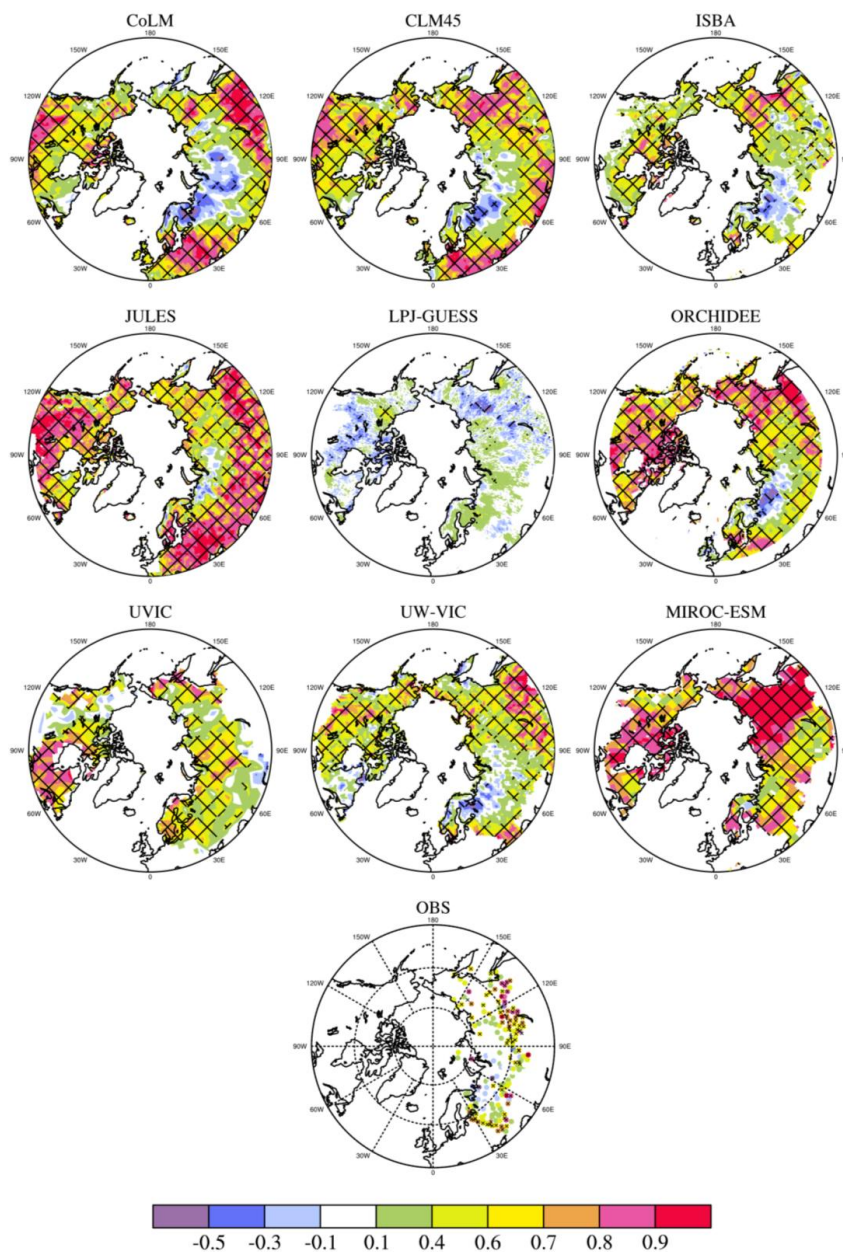


1
2

3 **Figure 2.** Conditional probability density functions (PDFs) of ΔT (K), the difference between
4 soil temperature at 20 cm depth and air temperature for different snow depth and air
5 temperature regimes (color) for winter 1980-2000.



30

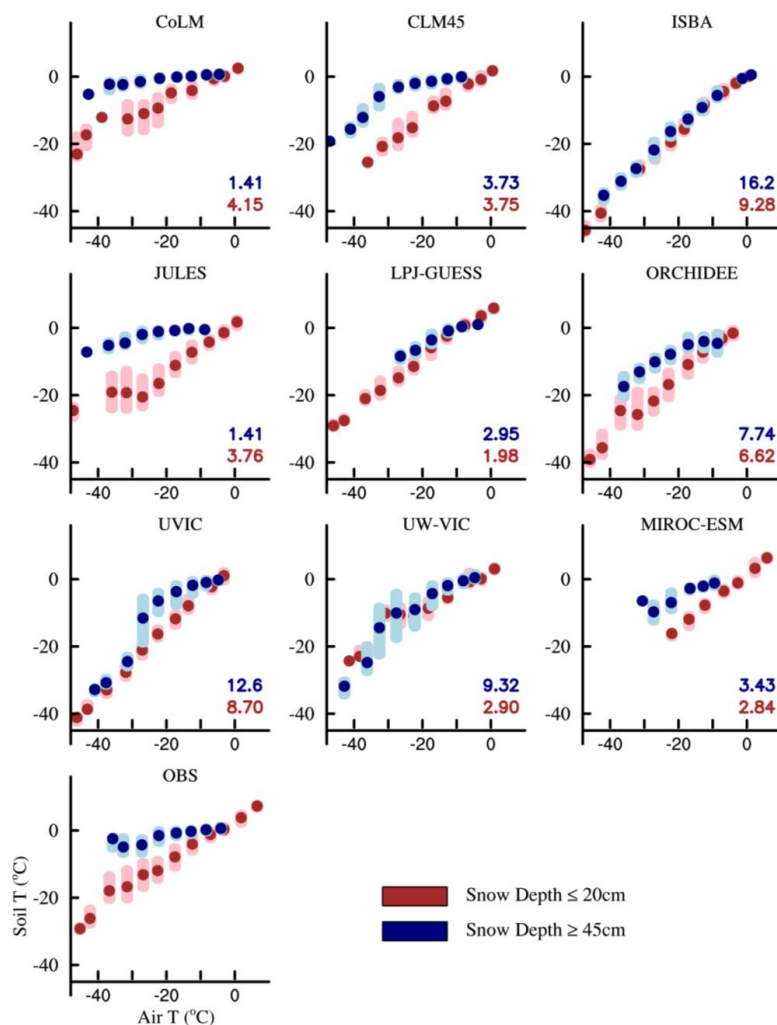


1
2
3
4
5

Figure 3. Spatial maps of the correlation coefficients between snow depth and ΔT , the difference between soil temperature at 20 cm depth and air temperature for winter 1980-2000. Regions with greater than 95% significance are hashed.



31

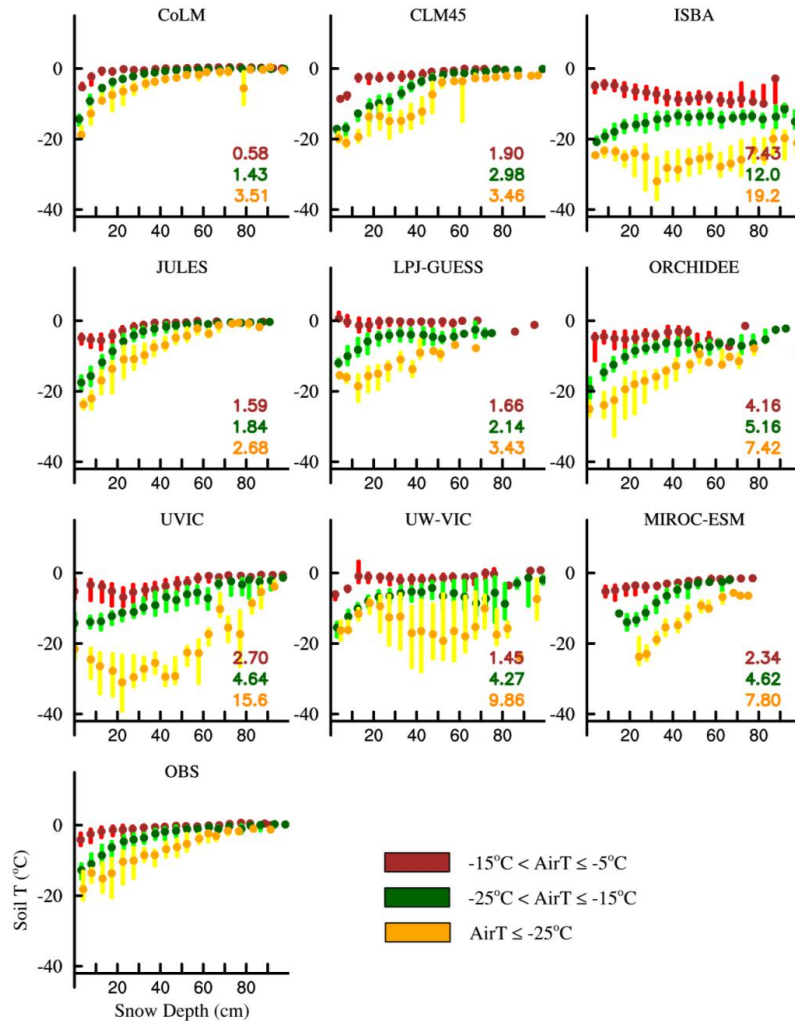


1
 2

3 **Figure 4.** Variation of soil temperature at 20 cm depth (°C) with air temperature (°C) for
 4 winter 1980-2000. The dots represent the medians of 5 °C air temperature bins and the upper
 5 and lower bars indicate the 25th and 75th percentiles, calculated from all Russian station grid
 6 points (n=268) and 21 individual winters. The numbers in each model panel indicate the
 7 RMSE between the observed and modeled relationship. Color represents different snow depth
 8 regimes.



32

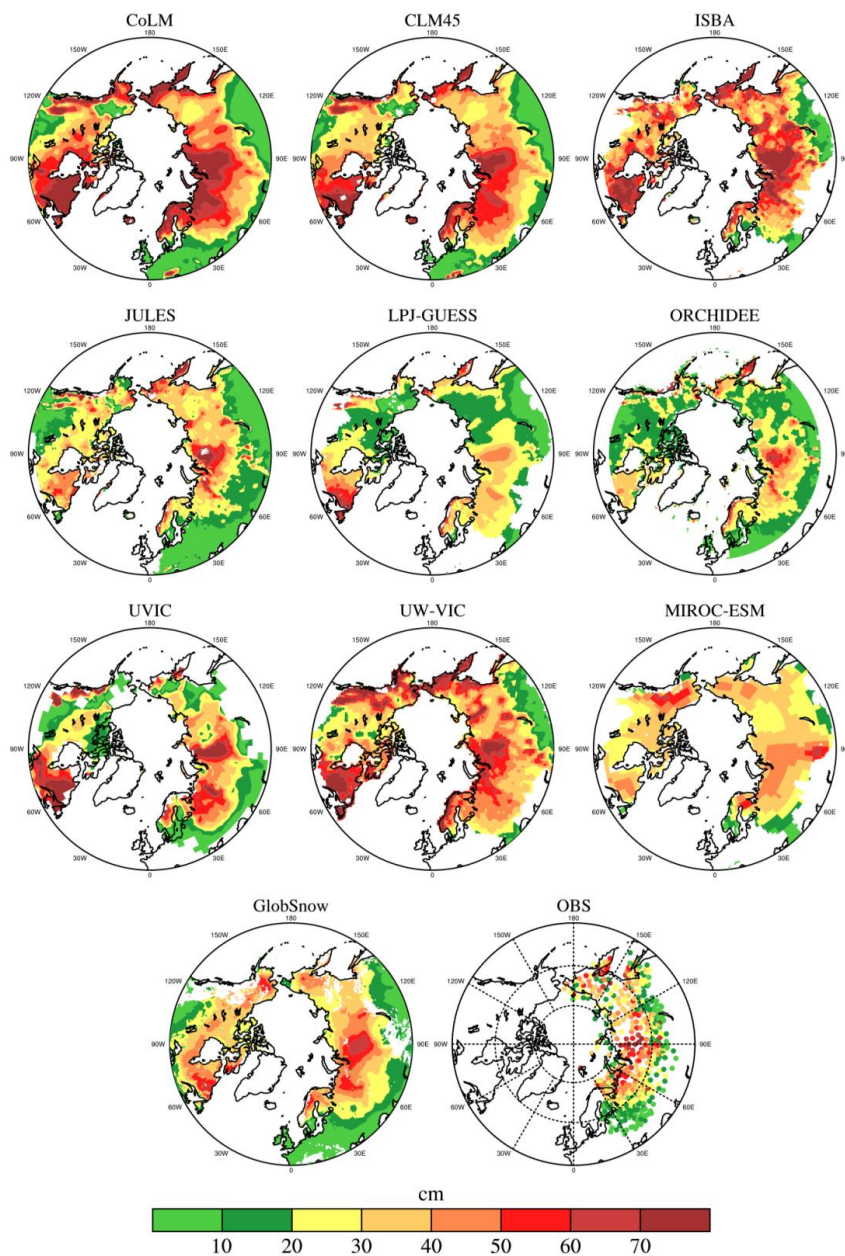


1
 2

3 **Figure 5.** Variation of soil temperature at 20 cm depth (°C; y axis) with snow depth (cm) for
 4 winter 1980-2000. The dots represent the medians of 5 cm snow depth bins and the upper and
 5 lower bars indicate the 25th and 75th percentiles, calculated from all Russian station grid points
 6 (n=268) and 21 individual winters. The numbers in each model panel indicate the RMSE
 7 between the observed and modeled relationship. Color represents different air temperature
 8 regimes.



33



1
2
3

Figure 6. Spatial maps of snow depth (cm) for winter 1980-2000.